

Design, Synthesis, and Antileishmanial Evaluation of 2-Aminothiophene Derivatives: Exploring New Drug Candidates for Leishmaniasis Treatment

Wei Zhang^{1*}, Mei Liu¹, Chen Hao²

¹Department of Pharmaceutical Sciences, School of Pharmacy, Peking University, Beijing, China.

²Department of Drug Design, Faculty of Pharmacy, Fudan University, Shanghai, China.

*E-mail ✉ wei.zhang@outlook.com

Received: 28 August 2022; Revised: 03 December 2022; Accepted: 06 December 2022

ABSTRACT

Leishmaniasis, classified by the World Health Organization as one of the 20 neglected tropical diseases, impacts around 12 million individuals across four continents and poses significant challenges to public health. The limited treatment choices, compounded by issues of drug toxicity and growing resistance to existing medications, underscore the critical need for novel therapeutic agents. This study seeks to deepen understanding of the key structural elements driving the anti-leishmanial activity in derivatives of 2-aminothiophene. To achieve this, a series of novel molecules were designed and prepared, incorporating targeted alterations at positions 3, 4, and 5 on the thiophene core, along with bioisosteric replacement of sulfur with selenium. Multiple derivatives of 2-aminothiophene (2-AT) and the corresponding 2-aminoselenophene (2-AS) analogs were prepared in sequence using the Gewald multicomponent reaction. These compounds were subsequently tested in vitro to assess their inhibitory effects on *Leishmania amazonensis* parasites and their potential toxic impact on mammalian macrophages. Various compound libraries were successfully generated, revealing specific structural trends that enhance potency. Notably, several analogs exhibited IC₅₀ values under 10 μM. Key insights include the dispensability of a cyano substituent at position 3; the critical role of cycloalkyl or piperidinyl substituents at positions 4 and 5, where chain length and type significantly influence efficacy; and the beneficial effect of sulfur-to-selenium bioisosteric exchange, which improved activity while preserving low cytotoxicity. Collectively, the results reinforce the promising outlook for 2-aminothiophene scaffolds as sources of viable anti-leishmanial candidates and provide valuable guidance for optimizing future compounds to address the ongoing challenges posed by leishmaniasis more effectively.

Keywords: Leishmaniasis, 2-aminothiophene, Drug design, Bioisosterism, Pharmacomodulation

How to Cite This Article: Zhang W, Liu M, Hao C. Design, Synthesis, and Antileishmanial Evaluation of 2-Aminothiophene Derivatives: Exploring New Drug Candidates for Leishmaniasis Treatment. *Pharm Sci Drug Des*. 2022;2:265-81. <https://doi.org/10.51847/UUpHVLyHcz>

Introduction

Leishmaniasis encompasses a spectrum of vector-transmitted parasitic infections triggered by protozoans belonging to the *Leishmania* genus, posing a major threat to public health across numerous tropical and subtropical areas. The World Health Organization (WHO) classifies it among the 20 neglected tropical diseases (NTDs) [1], manifesting in three primary clinical variants—visceral, mucocutaneous, and cutaneous—that occur endemically in nearly 100 nations spanning four continents, with roughly 12 million affected individuals and a global population at risk where one in eight people could potentially contract the infection [1-3].

The diverse clinical presentations of leishmaniasis vary in their immune-related pathology, severity, and mortality risks, largely determined by the specific *Leishmania* species involved [4]. Transmission to mammalian hosts, such as humans and canines, primarily happens via bites from infected female sandflies, with *Phlebotomus* species predominant in the Old World and *Lutzomyia* in the New World [5, 6].

Approximately 20 *Leishmania* species are responsible for cutaneous leishmaniasis (CL), notably including *L. major*, *L. tropica*, *L. amazonensis*, *L. braziliensis*, *L. guyanensis*, and *L. mexicana* [3, 6]. While not the deadliest

form (unlike untreated visceral leishmaniasis, which can be lethal), CL is the most common variant and carries substantial social burden due to the disfiguring ulcers and permanent scars it produces, leading to profound physical disfigurement and emotional distress for those affected [7, 8].

Despite the widespread impact and extensive research efforts aimed at managing this condition, no reliable vaccines have been developed to date [9-11], controlling the insect vector continues to present major obstacles [12], and advancements in pharmacological treatments have stagnated over recent decades [3, 13, 14].

The existing therapeutic options remain restricted and dated, relying mainly on pentavalent antimonials (such as Glucantime and Pentostam) as primary choices, supplemented by liposomal amphotericin B (AmBisome®), pentamidine, paromomycin, and miltefosine (IMPAVIDO®), the sole oral agent. These medications are hampered by drawbacks including high toxicity, severe adverse reactions, prolonged elimination times, elevated expenses, extended administration periods, and the rising incidence of drug-resistant parasites due to prolonged usage [3, 13, 15]. Such challenges emphasize the pressing requirement for identifying and creating novel, more efficacious and tolerable chemotherapeutic agents for leishmaniasis [3, 16, 17].

Within this framework, our team has focused on exploring novel anti-leishmanial agents derived from 2-aminothiophene scaffolds. Derivatives of 2-aminothiophene (2-AT) are recognized as versatile core structures in medicinal chemistry for developing molecules with biological activity, as highlighted in multiple contemporary review publications [18-21].

In relation to leishmaniasis, an initial investigation from our group demonstrated the anti-leishmanial properties of ten 2-AT compounds against *L. amazonensis* [22]. Among these, three stood out—SB-44, SB-83, and SB-200 (**Figure 1**)—displaying IC_{50} values of 7.37, 3.37, and 3.65 μ M against promastigotes and EC_{50} values of 15.82, 18.5, and 20.09 μ M against amastigotes, respectively, outperforming the standard drug meglumine antimoniate. This work suggested that the activity might involve an immunomodulatory pathway and pointed to the beneficial role of an indole moiety attached to the 2-amino group.

Building on this, compound SB-83 underwent oral *in vivo* testing in Swiss mice infected with *L. amazonensis*. Following seven weeks of administration at doses of 50 and 200 mg/kg, SB-83 proved superior to meglumine antimoniate (administered intraperitoneally at 100 mg/kg), significantly reducing lesion size in the paws and lowering parasite burden in affected tissues, while showing no notable alterations in biochemical, hematological, or histopathological markers [23].

Encouraged by these outcomes, we prepared and evaluated a library of 32 hybrid compounds combining 2-aminothiophene with indole motifs, varying the fused cycloalkyl ring size at thiophene positions C-4 and C-5 (ranging from 5- to 8-membered rings) and altering substituents (methyl, methoxyl, cyano, nitro) and their locations (C4', C5', C7') on the indole portion [24]. Over half of these hybrids (18 molecules) showed strong inhibitory effects on promastigotes, with IC_{50} values under 15.0 μ M, surpassing the activity and safety profiles of reference antimonials (trivalent and pentavalent, with IC_{50} of 12.7 and 87.7 μ M, respectively). The top performers were TN8-7, TN6-1, and TN7 (**Figure 1**), achieving IC_{50} values of 5.8, 7.2, and 10.0 μ M, respectively. These agents also effectively suppressed growth in a trivalent antimony (Sb^{3+})-resistant *L. amazonensis* strain (e.g., TN8-7: IC_{50} of 7.8 μ M in resistant vs. 5.8 μ M in sensitive strains, with no significant difference), indicating potential utility against resistant infections.

Findings from this effort revealed that the type and placement of substituents on the indole ring influence anti-*Leishmania* potency, with the 5' position emerging as particularly advantageous. Furthermore, enlarging the fused cycloalkyl ring on the thiophene core enhanced activity, with the cycloocta[b]thiophene analogs exhibiting the most favorable characteristics.

Subsequently, two separate investigations employing varied computational drug design strategies were carried out to build upon these results, adopting a more quantitative perspective to further establish 2-aminothiophenes as promising anti-*Leishmania* therapeutic leads.

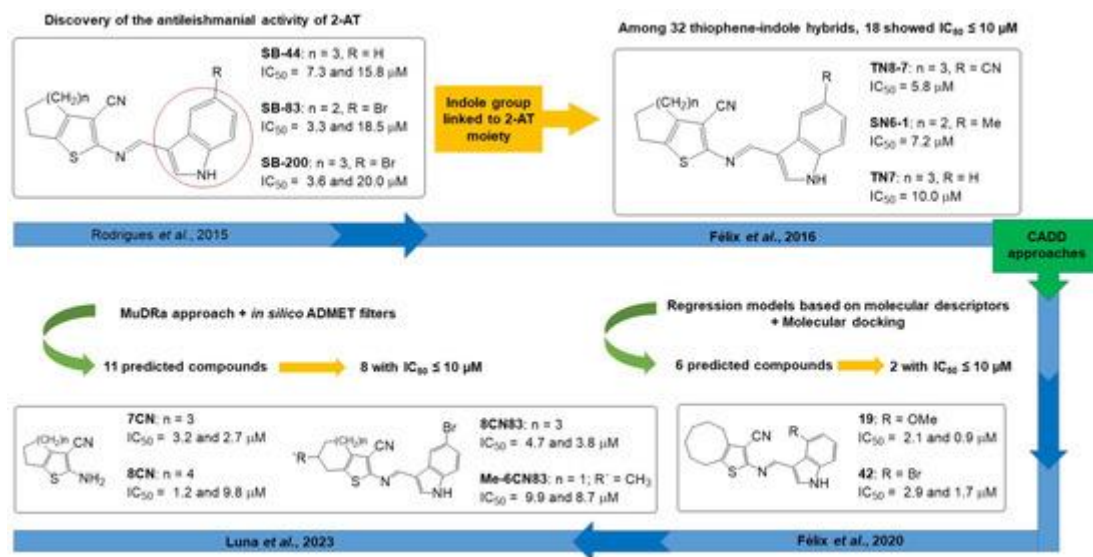


Figure 1. Chronological progression of drug discovery and development for 2-aminothiophenes exhibiting activity against leishmaniasis.

Inside the boxes are highlighted the lead compounds from each investigation. The reported IC_{50} values indicate the concentrations required for 50% inhibition of the promastigote and amastigote stages of *L. amazonensis*. The citations in the figure align with these references: Rodrigues *et al.*, 2015 [22]; Félix *et al.*, 2016 [24]; Félix *et al.*, 2020 [25]; and Luna *et al.*, 2023 [26].

In the initial relevant work, Félix *et al.* (2020) [25] employed a library of 92 2-aminothiophenes (2-AT) to develop predictive regression models relying on molecular descriptors computed with DRAGON 7.0 software, followed by statistical evaluation in MobyDigs v. 1.1. From these models, they chose 30 compounds displaying the most favorable forecasted IC_{50} values (expressed as pIC_{50}) and subjected them to molecular docking simulations targeting three key Leishmania enzymes: arginase, glycerol-3-phosphate dehydrogenase, and pyruvate kinase. Based on the docking outcomes, six candidates showing the highest promise for anti-Leishmania effects were prioritized, chemically prepared, and tested biologically against *L. amazonensis*. Among these six designed and produced molecules, two—designated as compounds 19 and 42—demonstrated strong antileishmanial effects on both parasite life-cycle stages, with IC_{50} values of 2.16 and $2.97 \mu M$ (promastigotes) and 0.9 and $1.71 \mu M$ (axenic amastigotes), respectively, along with selectivity indices (SI) of 52 and 75. These results surpassed the reference compound meglumine antimoniate (Sb+5), which had IC_{50} values of $70.33 \mu M$ (promastigotes) and $2.77 \mu M$ (amastigotes) and an SI of 1.01. Both active compounds share structural features, including the cycloocta[b]thiophene moiety and a substituent at the 4' position of the indole system (4'-OMe in 19 and 4'-Br in 42) (Figure 1).

In the subsequent investigation, Luna *et al.* (2023) [26] applied the Multi-Descriptor Read Across (MuDRA) methodology, integrated with computational ADMET and pharmacokinetic predictions via the pkCSM online platform as well as OSIRIS Data Explorer and DataWarrior v. 5.5 tools, to conduct virtual screening on a collection of 1862 structures sourced from the ChEMBL database, aiming to identify promising 2-AT candidates against *L. amazonensis*. This screening process yielded 11 2-aminothiophenes with favorable drug-like characteristics and over 70% predicted likelihood of inhibiting both parasite forms. These selected compounds were all synthesized, and eight of them (Figure 1) proved active against at least one parasite stage, exhibiting IC_{50} values below $10 \mu M$ and outperforming the reference meglumine antimoniate. Analysis of structure–activity relationships (SAR) indicated that: (1) indole groups attached to the amino site of the 2-AT core, particularly with a 5-bromo substitution, enhance but are not required for antileishmanial effects, and (2) the core Gewald products alone display inherent potential against the parasite.

These collective findings underscore the significant promise of 2-aminothiophene derivatives as antileishmanial agents and inspired further exploration of this core scaffold by designing, preparing, and biologically assessing novel analogs incorporating modifications at the C-3, C-4, and C-5 sites of the thiophene ring, alongside bioisosteric replacement of sulfur with selenium at the heterocyclic position.

Materials and Methods

Chemistry/synthesis

Preparation of 4-unsubstituted 2-aminothiophenes (1–3)

A round-bottom flask was charged with 2,5-dimethyl-2,5-dihydroxy-1,4-dithiane or 1,4-dithiane-2,5-diol (1 eq., 13.0 mmol) along with the appropriate α -activated acetonitrile (malononitrile, cyanoacetamide, or ethyl cyanoacetate; 2 eq.), and the mixture was dissolved in ethanol (15 mL). The flask was cooled in an ice bath, and morpholine (1 eq.) was added dropwise. After completion of the addition, stirring continued in the ice bath for 1 h, followed by heating at 50 °C for an additional 1–2 h. Progress was tracked by thin-layer chromatography (TLC). Upon cooling, the resulting precipitate was collected by filtration, washed with ethanol, and, if required, further purified by recrystallization from ethanol.

Preparation of 4,5-cyclosubstituted 2-aminothiophene-3-substituted derivatives and 2-aminocycloalkyl[b]selenophene-3-carbonitriles (7CN, 8CN, and 4–22)

The appropriate cyclic ketone (1 eq., 11.0 mmol), α -activated acetonitrile (1 eq.), and chalcogen (sulfur or selenium; 1 eq.) were combined in a round-bottom flask. Ethanol (30 mL) was added, the mixture was cooled in an ice bath, and morpholine (1.3 eq.) was introduced dropwise. Thirty minutes later, the reaction was warmed to 50–60 °C with continued stirring. Reactions were monitored by TLC and typically reached completion in 3–48 h. For most products, cooling induced precipitation, which was isolated by filtration and rinsed with cold ethanol. Additional purification, when needed, involved recrystallization from ethanol or standard silica gel column chromatography using hexane/ethyl acetate gradients.

Compounds 8CN and 6 initially afforded dark oils; solid forms were obtained by dissolving the material in 1:1 ethanol/water and refrigerating for several days.

For the selenophene analog 12, the crude reaction mixture was cooled to room temperature, treated with activated charcoal for 15 min to remove residual selenium, and filtered through celite under vacuum. The filtrate was concentrated to a dark liquid, which underwent liquid–liquid extraction with dichloromethane and water. Concentration of the organic layer yielded a viscous residue that was taken up in diethyl ether; cooling promoted solidification. Final purification was achieved by recrystallization from isopropanol, furnishing a brownish-red solid.

Deprotection of 2-amino-6-(N-Boc-piperidinyl)[b]thiophene-3-carbonitrile (17)

Compound 17 (1 eq., 0.71 mmol) was dissolved in a cooled (ice bath) 8:2 mixture of dichloromethane/trifluoroacetic acid (7.1 mL) and stirred for 20 min. Reaction progress was followed by TLC. Upon completion, volatiles were removed under reduced pressure to give a solid residue, which was recrystallized from ethanol to yield compound 23 as amorphous crystals.

Preparation of 2-Aminothiophene-5-Bromoindole-3-Carboxaldehyde Hybrids (SB-83, SB-200, 8CN83, Me-6CN83, and 25–31)

The appropriate Gewald adducts (7CN, 8CN, 4–6, 13–17, and 23; 1 eq.) and 5-bromoindole-3-carboxaldehyde (1 eq.) were combined in a round-bottom flask and dissolved in ethanol (5 mL). Acetic acid (10 drops) was added as catalyst, and the mixture was stirred at room temperature while monitoring by TLC. The desired products precipitated directly from the medium and were collected by filtration followed by rinsing with cold ethanol.

Preparation of 2-aminoselenophene-indole hybrids (32–40)

Gewald adduct 14 (1 eq., 1.1 mmol) and the corresponding substituted indole-3-carboxaldehyde (1 eq.) were placed in a round-bottom flask and dissolved in ethanol (5 mL). Acetic acid (10 drops) was added, and the reactions were stirred at room temperature with TLC monitoring. Upon completion, the precipitated products were isolated by filtration and washed with cold ethanol.

Confirmation of structures for the synthesized compounds

The identities of compounds 1 [27]; 2 and 3 [28]; 4 [29]; 5 and 7CN [30]; 8CN [31]; 7 [32]; 8 and 19 [33]; 9–11 [34]; 12 [35]; 13 and 17 [36]; 14 and 16 [37]; 15 [38]; 18 [39]; 20 [40]; 21 and 22 [41]; 23 [42]; 25, 8CN83, 26,

Me-6CN83, and 30 [26]; SB83 and SB200 [22] were verified through direct comparison of their NMR spectra with published data from the cited references.

The remaining novel substances (6, 24, 27–29, and 31–40) underwent full characterization to establish their molecular structures, with detailed descriptions of their physical properties.

Evaluation of antileishmanial activity and cytotoxicity in vitro

Maintenance of parasites and host cells

Experiments employed *Leishmania amazonensis* strains (IFLA/BR/67/PH8), sourced from the Oswaldo Cruz Foundation (FIOCRUZ) in Brazil. Promastigote stages were maintained in Schneider's insect medium at 26 °C within a BOD incubator. The medium was enriched with 20% fetal bovine serum (FBS) along with 1% penicillin (100 U/mL) and streptomycin (100 µg/mL) (referred to as complete Schneider's). Axenic amastigote stages were induced by shifting to Schneider's medium with 5% FBS, adjusted to pH 4.6, and incubated at 32 °C. In parallel, RAW 264.7 macrophage cells were grown in 750 cm² flasks using DMEM medium fortified with 10% FBS, 1% penicillin (100 U/mL), and 100 µg/mL streptomycin (complete DMEM), under conditions of 37 °C and 5% CO₂.

*Assessment of activity against promastigote and axenic amastigote stages of *L. amazonensis**

Inhibition of parasite proliferation was measured following the protocol outlined by Rodrigues *et al.* (2015) [22]. Log-phase cultures of promastigotes and axenic amastigotes (seeded at 1 × 10⁶ parasites/mL) were distributed in triplicate into 96-well plates with 100 µL of enriched Schneider's medium. Dilution series of the 2-amino-thiophene and 2-amino-selenophene compounds (ranging from 10.00 to 0.156 µM), as well as standard agents including meglumine antimoniate (500–40,000 µg/mL), amphotericin B (0.1–2 µM), and pentamidine (3.12–100 µM), were introduced. A negative control employed BNP. Plates were held in a BOD incubator (Eletrolab EL202, São Paulo, Brazil) at 26 °C for promastigotes or 32 °C for amastigotes over 72 hours. Subsequently, 10 µL of MTT solution (5 mg/mL) was added per well for colorimetric assessment of viability. After an additional 4-hour incubation, 50 µL of 10% sodium dodecyl sulfate was introduced to solubilize formazan crystals. Absorbance was measured using a microplate reader at primary wavelength 540 nm and reference 620 nm. The negative control (0.2% Schneider's with BNP) was defined as representing full viability.

Evaluation of cytotoxic effects on macrophages and calculation of selectivity index (SI)

Macrophage cultures (1 × 10⁶ cells in 100 µL complete DMEM) were seeded into 96-well plates. RAW 264.7 cells were sourced from ATCC (code TIB-71™). Plates were incubated at 37 °C with 5% CO₂ (Sanyo model COM-15A, Osaka, Japan) for 4 hours to allow attachment. Non-attached cells were eliminated by two rinses with pre-warmed DMEM (37 °C). The test compounds (2-amino-thiophene and 2-amino-selenophene series) were applied in dilution series from 400 to 25 µM, followed by 48-hour incubation. Viability was then assayed by adding 10 µL MTT (5 mg/mL final) and incubating for 4 hours. Plates were agitated for 30 minutes before reading absorbance at 550 nm (test) and 620 nm (reference). The control consisted of DMEM with 0.5% DMSO, taken as 100% viable macrophages. Selectivity indices were derived by dividing the CC₅₀ value for RAW 264.7 cells by the IC₅₀ or EC₅₀ obtained against the various *L. amazonensis* forms.

Evaluation of Chemical Stability

Stability testing was performed in triplicate using buffers at pH 1.2 (Clark-Lubs) and pH 7.4 (phosphate-buffered saline from commercial sources). Stock solutions of the 2-AT compounds were diluted to 1500 ng/mL from an intermediate acetonitrile stock (150 µg/mL). Samples were maintained at 37 °C in a shaking water bath within 2 mL microtubes. At designated intervals, 50 µL aliquots were withdrawn and placed into Max Recovery vials for instrumental analysis.

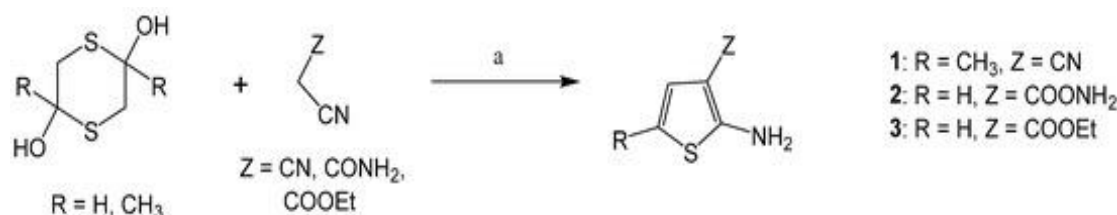
Analyses utilized an Acquity H-Class UPLC system (Waters, Milford, MA, USA) interfaced with a Xevo G2-S QToF high-resolution mass spectrometer equipped with ESI source (Waters, Milford, MA, USA). Data processing was handled via MassLynx 4.1 software. Separation was achieved on an HSS SB C18 column (2.1 × 100 mm, 1.7 µm) maintained at 35 °C, employing an 11-minute gradient elution with 2 µL injections. MS parameters, refined via direct infusion, included capillary voltage 3.5 kV, cone voltage 40 V, source temperature 150 °C, and desolvation gas at 500 L/h. Acquisition occurred in MSE mode, cycling low-energy (4 V) and ramped high-energy (10–40 V) collisions across the 0–11 minute runtime for thorough fragmentation profiling.

Results and Discussion

Synthesis

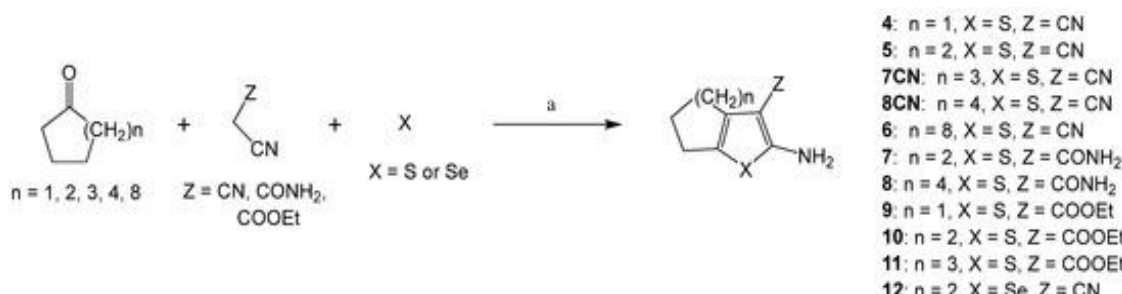
Initially, modified protocols of the classic Gewald reaction [43, 44] were applied to prepare the 2-aminothiophene (2-AT) and 2-aminoselenophene (2-AS) analogs described here.

Accordingly, for the preparation of compounds 1–3 (2-AT lacking substitution at position 4), the fourth variant of the Gewald reaction was utilized. This involved condensation of 1,4-dithiane-2,5-diol equivalents with α -activated nitriles (such as malononitrile, ethyl cyanoacetate, or cyanoacetamide) under basic conditions in ethanol (**Scheme 1**).

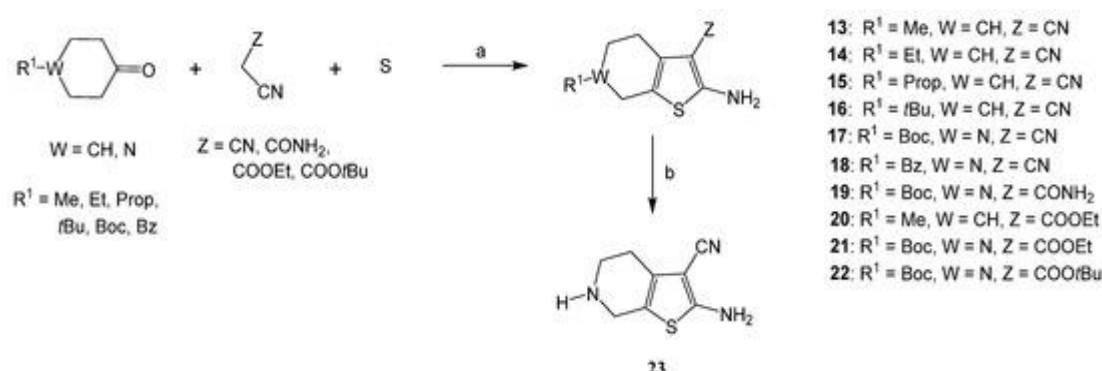


Scheme 1. Preparation of 2-aminothiophene (2-AT) involved treating derivatives of 1,4-dithiane-2,5-diol with morpholine in ethanol under reflux conditions for 2–3 hours (condition a).

The remaining Gewald products were prepared through the combination of various α -cyano-activated nitriles (such as malononitrile, ethyl cyanoacetate, tert-butyl cyanoacetate, or cyanoacetamide) with different cyclic ketones—including cyclopentanone, cyclohexanone, cycloheptanone, cyclooctanone, and cycloundecanone for products 4–12, 7CN, and 8CN; 4-alkyl-substituted cyclohexanones for products 13–16 and 20; N-Boc-protected piperidin-4-one for products 17, 19, 21, and 22; and N-benzylpiperidin-4-one for product 18—along with elemental sulfur or selenium in a basic ethanol solution. Product 23 was generated via removal of the Boc protecting group from product 17 employing a dichloromethane–trifluoroacetic acid mixture (8:2 ratio) (**Schemes 2 and 3**).

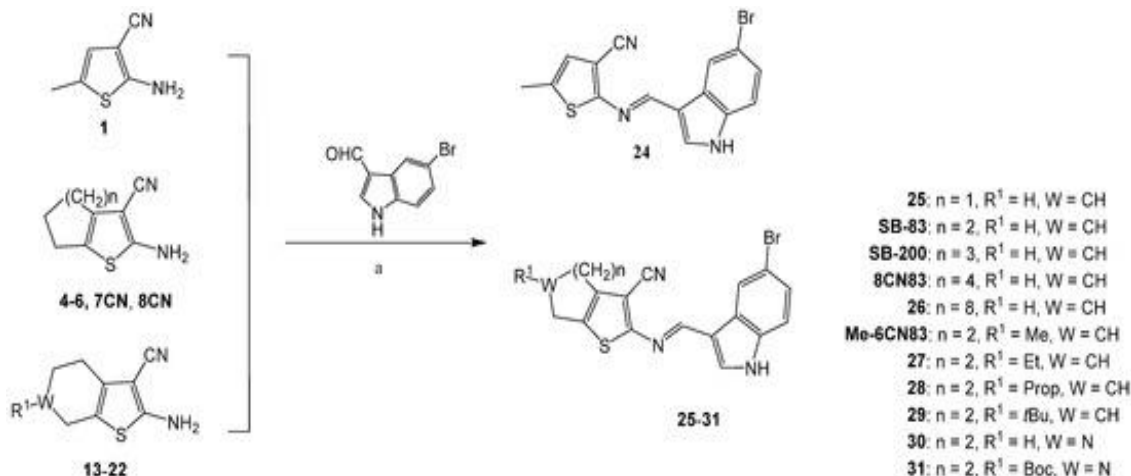


Scheme 2. Preparation of 2-aminothiophenes and 2-aminoselenophenes via the Gewald reaction: (a) morpholine, ethanol, heating under reflux, 4–48 hours.

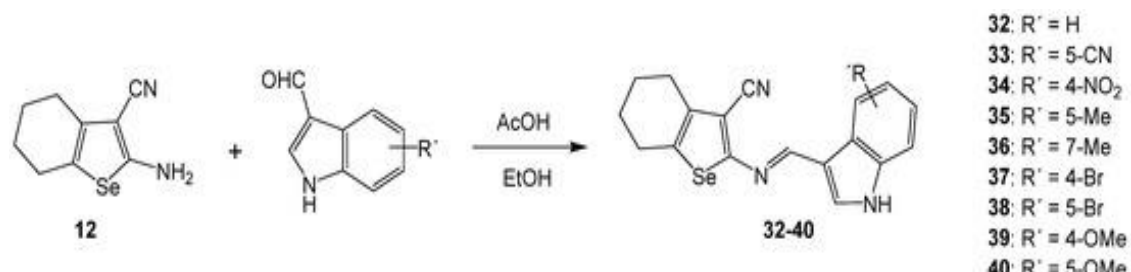


Scheme 3. Preparation of 2-aminothiophene (2-AT) via the Gewald reaction, starting with 4-alkylcyclohexanones, 4-N-benzyl-piperidone, and 4-Boc-piperidone.

The process involves (a) refluxing with morpholine and ethanol for 3–22 hours, followed by (b) treatment with a mixture of CH_2Cl_2 and TFA (8:2) at a temperature range of 0–5 °C for 20 minutes. Condensation reactions of 5-bromoindole-3-carboxaldehyde with 2-aminothiophenes yield a series of 2-aminothiophene-indole hybrids (24–31, SB-83, SB-200, 8CN83, and Me-6CN83) as shown in **Scheme 4**. Similarly, the condensation of substituted-indole-3-carboxaldehyde with 2-aminoselenophene 12 leads to the formation of 2-aminoselenophene-indole hybrids (32–40), as depicted in **Scheme 5**, following the method outlined in prior studies [22, 26].



Scheme 4. Synthesis of 2-aminothiophene-5-bromoindole hybrids, where the reaction is carried out by refluxing a mixture of ethanol and acetic acid for a duration of 2–24 hours.



Scheme 5. Synthesis of 2-Aminoselenophene-Indole Hybrids.

The target compounds were prepared using ethanol as solvent in the presence of acetic acid under reflux conditions overnight.

Following purification and assessment of their physicochemical properties, the structures of all novel compounds were verified using Nuclear Magnetic Resonance spectroscopy (^1H NMR, ^{13}C NMR, and DEPT) as well as High-Resolution Mass Spectrometry (HRMS). Previously reported compounds were resynthesized, and their identities were confirmed by comparison of physicochemical data and ^1H NMR spectra with literature values.

Pharmacomodulation study

Influence of cycloalkyl substituents at C-4/C-5 positions

Drawing from prior findings, the initial focus was to investigate the impact of alkyl and cycloalkyl groups attached to the C-4 and C-5 positions of the selenophene ring on the antipromastigote and antiamastigote activities against *Leishmania amazonensis*, while maintaining a fixed 5'-bromo-indole moiety. To this end, twelve compounds were synthesized and biologically evaluated. Their chemical structures, along with the corresponding IC_{50} (against parasites) and CC_{50} (cytotoxicity) values, are summarized in **Table 1**.

Table 1. Chemical structures, anti-Leishmania activity against promastigotes and axenic amastigotes of *L. amazonensis*, and cytotoxicity in macrophages of 5-bromoindole 2-aminothiophene hybrid derivatives (IC_{50} and CC_{50} values in μM).

Compound	Chemical Structures	IC_{50}		CC_{50}
		Promastigotes	Amastigotes	
24		>10.0	>10.0	n.t.
25 *		>10.0	>10.0	n.t.
SB-83 [#]		3.37	18.50	113.4
SB-200 [#]		3.65	20.09	32.0
8CN83 *		4.75	3.80	>100
26 *		>10.0	>10.0	n.t.
Me-6CN83 *		9.90	8.72	>100
27		>10.0	>10.0	n.t.
28		8.12	>10.0	n.t.
29		>10.0	>10.0	n.t.
30 *		>10.0	>10.0	n.t.

31		>10.0	>10.0	n.t.
Meglumine antimoniate	70.33	2.7	2.7	
Amphotericin B	0.17	0.23	0.18	

* Compounds published in Luna *et al.* (2023) [26]; [#] Compounds published in Rodrigues *et al.* (2015) [22]; n.t. = not tested.

According to **Table 1**, all compounds deemed active ($IC_{50} \leq 10.0 \mu\text{M}$) against at least one life-cycle stage of *L. amazonensis* exhibited superior antileishmanial potency compared to the reference drug pentavalent antimony (meglumine antimoniate) but inferior potency compared to amphotericin B (AmpB). Nevertheless, despite their lower activity relative to AmpB, these active compounds displayed significantly reduced cytotoxicity and a markedly higher therapeutic index.

These initial findings reinforce the observations previously reported by Luna *et al.* (2023) [26] and demonstrate that the nature of the substituent at the C-4 and C-5 positions of the selenophene ring plays a key role in modulating the antipromastigote and antimastigote activities of this compound class.

Removal of the cycloalkyl ring fused to the C-4 and C-5 positions, as seen in compound 24 (bearing only a methyl group at C-5), led to complete loss of antileishmanial activity, suggesting that the presence of a fused cycloalkyl moiety is essential for biological activity.

With respect to the size of the fused cycloalkyl ring, there appear to be optimal limits for retaining antileishmanial potency. Smaller five-membered rings (compound 25) and larger twelve-membered rings (compound 26) were inactive against both parasite forms. In contrast, fused 6-, 7-, and 8-membered rings—as exemplified by SB-83, SB-200 (previously described by Rodrigues *et al.* (2015) [22]), and 8CN83, respectively—displayed activity.

Among these, compound 8CN83 (with an 8-membered ring) emerged as the most promising against both parasite stages, showing the lowest IC_{50} value against the amastigote form ($IC_{50} = 3.8 \mu\text{M}$) while exhibiting no cytotoxicity up to 100 μM . This activity profile aligns with the findings reported by Félix *et al.* (2016) [24]. We hypothesize that these ring-size constraints may reflect an optimal spatial fit for interaction with biological targets and/or favorable physicochemical properties such as solubility or logP.

Bioisosteric replacement of a methylene (-CH₂-) group in the 6-membered ring compound SB-83 with an amine (-NH) in compound 30 proved detrimental, resulting in complete abolition of activity. This indicates that introduction of a hydrogen-bond donor in this region of the molecule is unfavorable for antileishmanial potency. Finally, introduction of alkyl substituents at the C-6 position of the tetrahydrobenzo[b]selenophene core of SB-83—methyl (Me-6CN83), ethyl (27), propyl (28), and tert-butyl (29)—was tolerated but did not enhance activity. Two of these derivatives (Me-6CN83 and 28) retained antileishmanial activity with IC_{50} values below 10 μM ; however, these were higher than those of the unsubstituted parent compound SB-83. Similarly, incorporation of a Boc protecting group in compound 31 provided no improvement over its N-unsubstituted counterpart (compound 30).

Chemical stability assay

The encouraging antileishmanial results obtained for several 2-aminoselenophene derivatives prompted chemical stability studies to assess potential metabolic degradation pathways. Five active compounds (TN8-1, TN8-2, SB-44, SB-83, and SB-200) were therefore selected for these experiments.

Preliminary in silico prediction using Zeneth software (Lhasa Limited, Version 7.1.3) indicated that the imine functionality was susceptible to hydrolysis at both pH 1.2 and 7.4, with more extensive degradation anticipated under acidic conditions.

Experimental stability testing in buffered solutions at pH 1.2 and 7.4 confirmed the formation of degradation products, consistent with the known lability of imine linkages. This observation parallels literature reports on imine-containing conjugates, such as those linking amphotericin to polyethylene glycol carriers, where minimal degradation (<5% over 24 h) occurred at alkaline pH, but rapid cleavage and drug release were observed at pH 5.5 (half-life <5 min) [45]. In the present study, degradation was too rapid at the tested pH values to allow half-life calculation.

The resulting degradation products (metabolites) were identified by UPLC-MS/MS analysis, revealing mass-to-charge (m/z) peaks corresponding to the original synthetic precursors: the 2-aminoselenophene Gewald adducts and the substituted indole components (**Figure 2**).

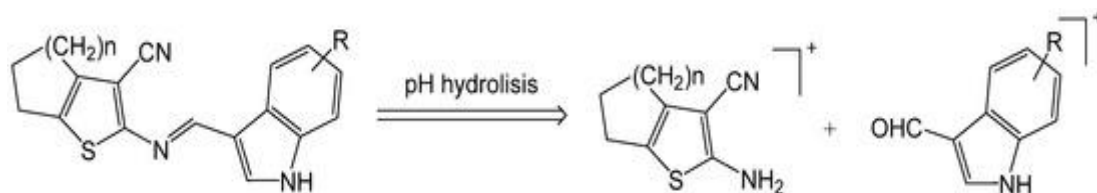


Figure 2. Synthetic Precursors Detected by UPLC-MS/MS during Chemical Stability Testing

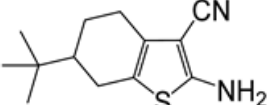
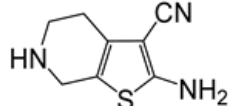
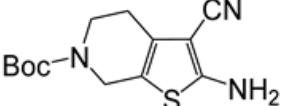
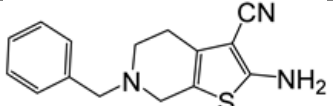
The figure illustrates the synthetic precursors identified via UPLC-MS/MS analysis following chemical stability assays conducted in buffer solutions at pH 1.2 and 7.4.

Influence of the absence of the indole substituent

In light of the stability data, and given that all 2-aminoselenophene derivatives listed in **Table 2** were prepared using the same indole aldehyde (5-bromoindole-3-carboxaldehyde), the variations observed in their IC₅₀ values highlight that modifications to the selenophene ring significantly influence the modulation of antileishmanial activity.

Table 2. Antileishmanial activity of Gewald adducts (2-aminothiophenes) and reference drugs against promastigotes and axenic amastigotes forms of *L. amazonensis* and cytotoxicity in macrophages (IC₅₀ and CC₅₀ values in μM).

Compound	Chemical Structures	IC ₅₀		CC ₅₀
		Promastigotes	Amastigotes	
1		>10.0	>10.0	n.t.
4		>10.0	>10.0	n.t.
5 *		>10.0	n.t.	125.40
7CN *		3.14	2.79	99.52
8CN *		1.20	2.60	43.90
13		>10.0	>10.0	n.t.
14		>10.0	>10.0	n.t.
15		9.2	9.3	n.t.

Compounds	Chemical Structures	IC ₅₀ Promastigotes	IC ₅₀ Amastigotes	CC ₅₀
16		>10.0	>10.0	n.t.
23		>10.0	>10.0	n.t.
17		8.61	>10.0	n.t.
18		>10.0	>10.0	n.t.
Meglumine antimoniate		58.9	2.7	44.9
Amphotericin B		0.30	0.23	0.30

n.t. = not tested. * Antileishmanial data of compounds 5, 7CN, and 8CN were previously published [26].

To explore whether the simpler Gewald adducts (basic 2-aminoselenophene cores) might themselves exhibit antileishmanial effects, we undertook biological evaluation of these intermediates. Positive findings in this direction would support the concept that the corresponding 2-aminoselenophene-indole hybrids function as mutual prodrugs of one another. Accordingly, Gewald adducts 4, 5, 7CN, 8CN, 13–18, and 23 were prepared and tested for activity against *L. amazonensis* (**Table 2**).

The outcomes in **Table 2** largely mirror the trends seen in **Table 1** and provide strong support for the prodrug hypothesis involving the 2-aminoselenophene-indole hybrids. Specifically, **Table 2** reaffirms that lack of a fused cycloalkyl ring at the C-4/C-5 positions of the selenophene, as in compound 1, abolishes antileishmanial potency. It further corroborates that larger fused cycloalkyl rings enhance activity, with compound 8CN (incorporating an 8-membered ring) displaying the most favorable profile: IC₅₀ values of 1.2 μM against promastigotes and 2.6 μM against amastigotes.

Table 2 also confirms that alkyl groups at the C-6 position are generally tolerated without improving potency. Among these, only compound 15 achieved IC₅₀ values <10 μM against both parasite stages, consistent with the behavior of its hybrid counterpart 28 (**Table 1**). By contrast, compound 13 showed no activity, unlike its more potent hybrid derivative Me-6CN83. Replacement of the cyclohexyl moiety with a piperidinyl ring (compound 23) similarly failed to improve activity (IC₅₀>10 μM), aligning with observations for hybrid 30 in **Table 1**.

N-Substitution on the piperidinyl ring yielded mixed outcomes. A benzyl substituent (compound 18) rendered the compound inactive, whereas a tert-butyloxycarbonyl (Boc) group (compound 17) conferred moderate activity against promastigotes (IC₅₀ = 8.61 μM), making it superior to its corresponding inactive hybrid 31 (**Table 1**) (IC₅₀ >10 μM). Collectively, these data indicate that an unsubstituted secondary amine—which can serve as a hydrogen-bond donor—is detrimental to antileishmanial activity in this molecular region. However, appropriate N-protection or substitution can restore or even impart potency, suggesting promising opportunities for further optimization of substituents at this site.

Influence of substituents at the C-3 position

Having established that the core Gewald adducts themselves display antileishmanial properties, we extended the pharmacomodulation efforts to examine the consequences of varying functionality at the C-3 position. A series of Gewald adducts bearing either ester or amide groups at C-3 were therefore synthesized and assessed for activity against *L. amazonensis* (**Table 3**).

Table 3. Antileishmanial evaluation of 3-substituted Gewald adducts and reference drugs against the promastigotes and axenic amastigotes forms of *L. amazonensis* and cytotoxicity in macrophages (IC₅₀ and CC₅₀ values in μM).

Compounds	Chemical Structures	IC ₅₀		CC ₅₀
		Promastigotes	Amastigotes	

2		>10.0	>10.0	n.t.
7		>10.0	>10.0	n.t.
8		>10.0	>10.0	n.t.
19		9.35	>10.0	309.7
3		>10.0	>10.0	n.t.
9		>10.0	n.t.	n.t.
10		>10.0	n.t.	n.t.
11		>10.0	n.t.	n.t.
20		>10.0	n.t.	n.t.
21		3.1	2.9	220.83
22		6.52	8.35	194.56
Meglumine antimoniate		67.9	2.77	2.77
Anfotericina B		0.36	0.23	0.38

n.t.: not tested.

Analysis of **Table 3**, in comparison with the data from **Table 2**, reveals that substitution of the C-3 carbonitrile (-CN) group with either a primary carboxamide (-CONH₂) (compounds 2, 7, and 8) or carboxylate ester (-COOR) (compounds 3, 9–11, and 20) is generally detrimental to the antileishmanial potency of the Gewald adducts. None of these modified compounds exhibited activity below the predefined threshold ($IC_{50} \leq 10 \mu M$), and the change led to a total abolition of activity in the case of compound 7CN (which bears a 3-CN group) against both promastigote and amastigote forms of *L. amazonensis*.

Positive pharmacomodulation upon replacement of the C-3 carbonitrile with carboxamide or carboxylate functionality was observed only in the subset of 2-aminoselenophenes featuring an N-Boc-piperidinyl unit fused at C-4/C-5 (compounds 19, 21, and 22). Replacement of the nitrile in compound 17 with an amide in compound 19 preserved antipromastigote activity ($IC_{50} 8.61 \mu M$ versus $9.35 \mu M$).

More notably, introduction of carboxylate esters (compounds 21 and 22) markedly improved potency against both parasite stages relative to the nitrile-bearing analog 17, demonstrating a highly beneficial effect of this modification. The enhancement was most striking for the ethyl ester derivative 21, which achieved IC_{50} values of $3.1\ \mu M$ (promastigotes) and $2.9\ \mu M$ (amastigotes). Switching the ethyl group to a bulkier tert-butyl in compound 22 reduced activity more than twofold ($IC_{50} = 6.52\ \mu M$ and $8.35\ \mu M$ against promastigotes and amastigotes, respectively), suggesting steric or volumetric constraints on the alkyl chain of the ester moiety.

Influence of sulfur–selenium bioisosterism

The final structural variation examined the role of the heteroatom in the ring by conducting a classical S/Se bioisosteric replacement, thereby generating novel 2-aminoselenophene-indole hybrids to assess the impact of selenium versus sulfur on antileishmanial activity.

These newly synthesized 2-aminoselenophene-indole compounds were evaluated for their antipromastigote activity against *L. amazonensis* (**Table 4**) and directly compared with the corresponding 2-aminothiophene-indole hybrids reported in our earlier investigations [22, 24].

Table 4. Anti-promastigote activity of 2-aminoselenophene-indole hybrids and reference drugs against *L. amazonensis* and cytotoxicity in macrophages (IC_{50} and CC_{50} values in μM).

Compounds	R	Anti-Promastigotes		Cytotoxicity	SI
		IC_{50}	CC_{50}		
32	-H	>10.0	n.t.		-
33	5-CN	9.32	203.46	21.83	
34	4-NO ₂	2.14	189.37	88.49	
35	5-CH ₃	>10.0	n.t.		-
36	7-CH ₃	2.92	185.89	63.66	
37	4-Br	4.50	241.70	53.71	
38	5-Br	3.49	238.94	68.45	
39	4-OCH ₃	2.15	178.46	83.00	
40	5-OCH ₃	>10.0	n.t.		-
Amphotericin B		0.36	0.38	1.10	
Pentamidine		42.32	293.79	6.90	

n.t.: Not tested; SI = CC_{50}/IC_{50} .

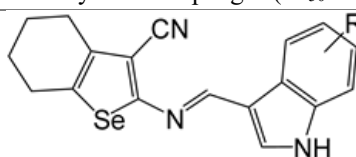
Examination of the results in **Table 4** reveals that six out of the nine 2-aminoselenophene derivatives exhibited inhibitory effects against the promastigote stage of *L. amazonensis* at concentrations below $10\ \mu M$. Compounds 32 (unsubstituted indole), 35 (5-methyl-indole), and 40 (5-methoxy-indole) remained inactive even at the maximum tested concentration.

The standout 2-aminoselenophene (2-AS) compounds were 34 (bearing a 4-NO₂ group), 36 (7-CH₃), 38 (5-Br), and 39 (4-OCH₃), all achieving IC_{50} values under $3.5\ \mu M$.

These findings reinforce the previously established critical role of the 5-bromoindole moiety (as in compound 38) in conferring antileishmanial potency [26], while also showing that various electron-donating and electron-withdrawing substituents at different positions on the indole ring are well tolerated, consistent with prior observations by Félix *et al.* (2016) [24].

The S/Se bioisosteric replacement in these 2-aminoselenophene series generally proved advantageous for antileishmanial efficacy, yielding derivatives with potency equal to or greater than that of their corresponding 2-aminothiophene counterparts.

Specifically, four 2-AS compounds—33 ($IC_{50} = 9.32\ \mu M$), 34 ($IC_{50} = 2.14\ \mu M$), 36 ($IC_{50} = 2.92\ \mu M$), and 39 ($IC_{50} = 2.15\ \mu M$)—demonstrated superior activity compared to their 2-aminothiophene analogs reported by Félix *et al.* (2016) [24]: TN6-7 ($IC_{50} = 14.2\ \mu M$), TN6-4 ($IC_{50} = 85.3\ \mu M$), TN6-3 ($IC_{50} = 100.8\ \mu M$), and TN6-2 ($IC_{50} = 17.9\ \mu M$).



Two additional 2-AS derivatives—32 ($IC_{50} > 10.0 \mu M$) and 38 ($IC_{50} = 3.49 \mu M$)—displayed comparable potency to their thiophene bioisosteres TN6 ($IC_{50} = 14.7 \mu M$) and SB-83 ($IC_{50} = 3.37 \mu M$). Only compound 35 ($IC_{50} > 10.0 \mu M$) was less active than its thiophene counterpart TN6-1 ($IC_{50} = 7.2 \mu M$).

Moreover, counter to expectations of heightened toxicity for organoselenium compounds [46, 47], all evaluated 2-AS derivatives exhibited excellent selectivity indices (SIs) between 21.83 and 83.00—substantially exceeding those of the standard agents amphotericin B and pentamidine (SI = 1.1 and 6.9, respectively). This profile positions them as promising candidates with a broad therapeutic window.

Notably, while the bioisosteric pair 38 and SB-83 showed similar antileishmanial potency, the selenophene analog 38 (SI = 68) afforded roughly double the safety margin of its thiophene counterpart SB-83 (SI = 33.6). Thus, the S/Se exchange not only maintained or enhanced antiparasitic activity but also lowered cytotoxicity.

Conclusion

This study provides an opportunity to further investigate the pharmacophore linked to the antileishmanial effects of 2-aminothiophene derivatives and to identify beneficial substitution patterns that can guide the design of novel compounds with enhanced activity. The findings that simpler Gewald adducts, which are synthetic precursors of 2-aminothiophene-indole hybrids, also exhibit biological activity support the hypothesis that these hybrids may function as reciprocal prodrugs.

The analysis of the substituent effect at C-3 on the anti-Leishmania activity revealed that substituting the carbonitrile group (-CN) with carboxamide (-CONH₂) or carboxylates (-COOR) generally reduces the activity, although this does not rule out the potential for further exploration of compounds with N-substituted amides. Additionally, the presence and size of cycloalkyl or piperidinyl chains at C-4/C-5 were found to influence the activity, with particular focus on cycloocta[b]thiophene derivatives (8-membered rings) showing a noteworthy role in modulating the antileishmanial activity.

Furthermore, the study emphasizes that the nitrogen substitution at the piperidinyl ring at C-4/C-5 is crucial for maintaining activity, which opens avenues for investigating different N-substitution patterns. Compounds featuring both N-piperidinyl substitutions and 3-carboxamide or 3-carboxylate groups also demonstrated enhanced pharmacomodulation.

The S-Se bioisosteric substitution strategy proved highly advantageous in developing compounds that maintain or even surpass the antileishmanial efficacy of their 2-aminothiophene counterparts without significant cytotoxicity. This approach has yielded positive results in recent research, including the development of new anti-chagasic drugs [48] and adenosine A2A receptor inhibitors [49], and it also contributes to antioxidant activity while improving the lipophilicity of the molecules [47].

These targeted chemical modifications across different positions of the 2-aminothiophene scaffold suggest a rational approach for synthesizing new derivatives with enhanced potential, adhering to a Hit-to-Lead (H2L) optimization strategy.

Key recommendations from this study include considering the following for future compound designs: (1) sulfur-to-selenium substitution; (2) retaining carbonitrile at C-3; (3) incorporating large cycloalkyl chains, such as cycloocta[b]thiophene, at C-4/C-5; (4) alternatively, using N-substituted piperidinyl chains at C-4/C-5 in conjunction with carboxylate groups at C-3.

Finally, there is a pressing need to conduct drug target deconvolution studies, which are essential for identifying the primary targets of 2-aminothiophene derivatives. This would not only help clarify the mechanism of action but also provide valuable insights for target-based drug design (SBDD), guiding further synthesis efforts and the optimization of compound efficacy [50-52].

Acknowledgments: None

Conflict of Interest: None

Financial Support: None

Ethics Statement: None

References

1. World Health Organization. Leishmaniases. 2023. Available online: <https://www.who.int/news-room/fact-sheets/detail/leishmaniasis> (accessed on 29 September 2024).
2. Burza, S.; Croft, S.L.; Boelaert, M. Leishmaniasis. *Lancet* 2018, 392, 951–70.
3. Corman, H.N.; McNamara, C.W.; Bakowski, M.A. Drug Discovery for Cutaneous Leishmaniasis: A Review of Developments in the Past 15 Years. *Microorganisms* 2023, 11, 2845.
4. Roatt, B.M.; De Oliveira Cardoso, J.M.; De Brito, R.C.F.; Coura-Vital, W.; De Oliveira Aguiar-Soares, R.D.; Barbosa Reis, A. Recent advances and new strategies on leishmaniasis treatment. *Appl. Microbiol. Biotechnol.* 2020, 104, 8965–77.
5. Tabbabi, A. Review of Leishmaniasis in the Middle East and North Africa. *Afr. Health Sci.* 2019, 19, 1329–37.
6. DeWinter, S.; Shahin, K.; Fernandez-Prada, C.; Greer, A.L.; Weese, J.S.; Clow, K.M. Ecological determinants of leishmaniasis vector, *Lutzomyia* spp.: A scoping review. *Med. Vet. Entomol.* 2024, 38, 393–406.
7. Gurel, M.S.; Tekin, B.; Uzun, S. Cutaneous leishmaniasis: A great imitator. *Clin. Dermatol.* 2020, 38, 140–51.
8. Bennis, I.; Thys, S.; Filali, H.; De Brouwere, V.; Sahibi, H.; Boelaert, M. Psychosocial impact of scars due to cutaneous leishmaniasis on high school students in Errachidia province, Morocco. *Infect. Dis. Poverty* 2017, 6, 46.
9. Shital, S.; Madan, E.; Selvapandian, A.; Kumar Ganguly, N. An update on recombinant vaccines against leishmaniasis. *Indian. J. Med. Res.* 2024, 160, 323–37.
10. Kaye, P.M.; Mohan, S.; Mantel, C.; Malhame, M.; Revill, P.; Le Rutte, E.; Parkash, V.; Layton, A.M.; Lacey, C.J.N.; Malvolfi, S. Overcoming roadblocks in the development of vaccines for leishmaniasis. *Expert. Rev. Vaccines* 2021, 20, 1419–30.
11. Ghorbani, M.; Farhoudi, R. Leishmaniasis in humans: Drug or vaccine therapy? *Drug Des. Dev. Ther.* 2018, 12, 25–40.
12. Montenegro Quiñonez, C.A.; Runge-Ranzinger, S.; Rahman, K.M.; Horstick, O. Effectiveness of vector control methods for the control of cutaneous and visceral leishmaniasis: A meta-review. *PLoS Negl. Trop. Dis.* 2021, 15, e0009309.
13. Rodriguez, F.; Iniguez, E.; Pena Contreras, G.; Ahmed, H.; Costa, T.E.M.M.; Skouta, R.; Maldonado, R.A. Development of Thiophene Compounds as Potent Chemotherapies for the Treatment of Cutaneous Leishmaniasis Caused by *Leishmania major*. *Molecules* 2018, 23, 1626.
14. Sasidharan, S.; Saudagar, P. Leishmaniasis: Where are we and where are we heading? *Parasitol. Res.* 2021, 120, 1541–54.
15. Brannigan, J.A.; Wilkinson, A.J. Drug discovery in leishmaniasis using protein lipidation as a target. *Biophys. Rev.* 2021, 13, 1139–46.
16. Andrade-Neto, V.V.; Cunha-Junior, E.F.; Dos Santos Faioes, V.; Pereira, T.M.; Silva, R.L.; Leon, L.L.; Torres-Santos, E.C. Leishmaniasis treatment: Update of possibilities for drug repurposing. *Front. Biosci.* 2018, 23, 967–96.
17. Espada, C.R.; Ribeiro-Dias, F.; Dorta, M.L.; Pereira, L.I.A.; Carvalho, E.M.; Machado, P.R.; Schriefer, A.; Yokoyama-Yasunaka, J.K.U.; Coelho, A.C.; Uliana, S.R.B. Susceptibility to miltefosine in brazilian clinical isolates of *Leishmania* (Viannia) *braziliensis*. *Am. J. Trop. Med. Hyg.* 2017, 96, 656–9.
18. Duvauchelle, V.; Meffre, P.; Benfodda, Z. Green methodologies for the synthesis of 2-aminothiophene. *Environ. Chem. Lett.* 2023, 21, 597–621.
19. Duvauchelle, V.; Meffre, P.; Benfodda, Z. Recent contribution of medicinally active 2-aminothiophenes: A privileged scaffold for drug discovery. *Eur. J. Med. Chem.* 2022, 238, 114502.
20. Bozorov, K.; Nie, L.F.; Zhao, J.; Aisa, H.A. 2-Aminothiophene scaffolds: Diverse biological and pharmacological attributes in medicinal chemistry. *Eur. J. Med. Chem.* 2017, 140, 465–93.
21. Darwish, D.G.; El-Sherief, H.A.M.; Abdel-Aziz, S.A.; Abuo-Rahma, G.E.A. A decade's overview of 2-aminothiophenes and their fused analogs as promising anticancer agents. *Arch. Pharm.* 2024, 357, e2300758.

22. Rodrigues, K.A.; Dias, C.N.; Néris, P.L.; Rocha, J.C.; Scotti, M.T.; Scotti, L.; Mascarenhas, S.R.; Veras, R.C.; De Medeiros, I.A.; Keesen, T.S.; et al. 2-Amino-thiophene derivatives present antileishmanial activity mediated by apoptosis and immunomodulation in vitro. *Eur. J. Med. Chem.* 2015, 106, 1–14.

23. Rodrigues, K.A.D.F.; Silva, D.K.F.; Serafim, V.L.; Andrade, P.N.; Alves, A.F.; Tafuri, W.L.; Batista, T.M.; Mangueira, V.M.; Sobral, M.V.; Moura, R.O.; et al. SB-83, a 2-Amino-thiophene derivative orally bioavailable candidate for the leishmaniasis treatment. *Biomed. Pharmacother.* 2018, 108, 1670–8.

24. Félix, M.B.; De Souza, E.R.; De Lima, M.D.C.A.; Frade, D.K.G.; Serafim, V.L.; Rodrigues, K.A.D.F.; Néris, P.L.D.N.; Ribeiro, F.F.; Scotti, L.; Scotti, M.T.; et al. Antileishmanial activity of new thiophene-indole hybrids: Design, synthesis, biological and cytotoxic evaluation, and chemometric studies. *Bioorg. Med. Chem.* 2016, 24, 3972–7.

25. Félix, M.B.; De Araújo, R.S.A.; Barros, R.P.C.; De Simone, C.A.; Rodrigues, R.R.L.; De Lima Nunes, T.A.; Da Franca Rodrigues, K.A.; Junior, F.J.B.M.; Muratov, E.; Scotti, L.; et al. Computer-Assisted Design of Thiophene-Indole Hybrids as Leishmanial Agents. *Curr. Top. Med. Chem.* 2020, 20, 1704–19.

26. Luna, I.S.; Souza, T.A.; Da Silva, M.S.; Franca Rodrigues, K.A.D.; Scotti, L.; Scotti, M.T.; Mendonça-Junior, F.J.B. Computer-Aided drug design of new 2-amino-thiophene derivatives as antileishmanial agents. *Eur. J. Med. Chem.* 2023, 250, 115223.

27. Tayebjee, R.; Ahmadi, S.J.; Seresht, E.R.; Javadi, F.; Yasemi, M.A.; Hosseinpour, M.; Maleki, B. Commercial zinc oxide: A facile, efficient and eco-friendly catalyst for the one-pot three-component synthesis of multi-substituted 2-aminothiophenes via Gewald reaction. *Ind. Eng. Chem. Res.* 2012, 51, 14577–82.

28. Li, P.; Du, J.; Xie, Y.; Tao, M.; Zhang, W.-Q. Highly efficient polyacrylonitrile fiber catalysts functionalized by aminopyridines for the synthesis of 3-substituted 2-aminothiophenes in water. *ACS Sustain. Chem. Eng.* 2016, 4, 1139–47.

29. Wardakhan, W.W.; Samir, E.M. The reaction of cyclopentanone with cyanomethylene reagents: Novel synthesis of pyrazole, thiophene, and pyridazine derivatives. *J. Chem.* 2013, 2013, 427158.

30. Zhao, D.-D.; Li, L.; Fan, X.; Wu, Q.; Lin, X.-F. Bovine serum albumin-catalyzed one-pot synthesis of 2-aminothiophenes via Gewald reaction. *J. Mol. Catal. B Enzym.* 2013, 95, 29–35.

31. Arhin, F.; Bélanger, O.; Ciblat, S.; Dehbi, M.; Delorme, D.; Dietrich, E.; Dixit, D.; LaFontaine, Y.; Lehoux, D.; Liu, J.; et al. A new class of small molecule RNA polymerase inhibitors with activity against Rifampicin-resistant *Staphylococcus aureus*. *Bioorg. Med. Chem.* 2006, 14, 5812–32.

32. Hemdan, M.M.; El-Mawgoude, H.K.A. Uses of 1-(3-Cyano-4,5,6,7-tetrahydrobenzo[b]-thiophen-2-yl)-3-dodecanoylthiourea as a building block in the synthesis of fused pyrimidine and thiazine systems. *Chem. Pharm. Bull.* 2015, 63, 450–6.

33. Nallangi, R.; Samala, G.; Sridevi, J.P.; Yogeeswari, P.; Sriram, D. Development of antimycobacterial tetrahydrothieno [2,3-c]pyridine-3-carboxamides and hexahydrocycloocta[b]thiophene-3-carboxamides: Molecular modification from known antimycobacterial lead. *Eur. J. Med. Chem.* 2014, 76, 110–17.

34. Mojtabedi, M.M.; Abaee, M.S.; Mahmoodi, P.; Adib, M. Convenient synthesis of 2-aminothiophene derivatives by acceleration of Gewald reaction under ultrasonic aqueous conditions. *Synth. Commun.* 2010, 40, 2067–74.

35. Seck, P.; Thomae, D.; Perspicace, E.; Hesse, S.; Kirsch, G. Synthesis of new selenophene and thiazole analogues of the Tacrine series. *ARKIVOC* 2012, 3, 431–41.

36. Wang, T.; Huang, X.-G.; Liu, J.; Li, B.; Wu, J.-J.; Chen, K.-X.; Zhu, W.-L.; Xu, X.-Y.; Zeng, B.-B. An efficient one-pot synthesis of substituted 2-aminothiophenes via three-component Gewald reaction catalyzed by L-proline. *Synlett* 2010, 2010, 1351–4.

37. Xu, F.; Li, Y.; Xu, F.; Ye, Q.; Han, L.; Gao, J.; Yu, W. Solvent-free synthesis of 2-aminothiophene-3-carbonitrile derivatives using high-speed vibration milling. *J. Chem. Res.* 2014, 38, 450–2.

38. Shaabani, A.; Hooshmand, S.E.; Afaridoun, H. A green chemical approach: A straightforward one-pot synthesis of 2-aminothiophene derivatives via Gewald reaction in deep eutectic solvents. *Monatsh. Chem.* 2017, 148, 711–6.

39. Kaki, V.R.; Akkinepalli, B.R.; Deb, P.K.; Pichika, M.R. Basic ionic liquid [bmIm]OH-mediated Gewald reaction as green protocol for the synthesis of 2-aminothiophenes. *Synth. Commun.* 2015, 45, 119–26.

40. Katzman, B.M.; Perszyk, R.E.; Yuan, H.; Tahirovic, Y.A.; Sotimehin, A.E.; Traynelis, S.F.; Liotta, D.C. A novel class of negative allosteric modulators of NMDA receptor function. *Bioorg. Med. Chem. Lett.* 2015, 25, 5583–8.

41. Cruz, R.M.D.; Zelli, R.; Benhsain, S.; Cruz, R.M.D.; Siqueira-Júnior, J.P.; Décout, J.-L.; Mingeot-Leclercq, M.-P.; Mendonça-Junior, F.J.B. Synthesis and evaluation of 2-aminothiophene derivatives as *Staphylococcus aureus* efflux pump inhibitors. *ChemMedChem* 2020, 15, 716–25.

42. Mekheimer, R.A.; Ameen, M.A.; Sadek, K.U. Solar thermochemical reactions II¹: Synthesis of 2-aminothiophenes via Gewald reaction induced by solar thermal energy. *Chin. Chem. Lett.* 2008, 19, 788–90.

43. Gewald, K.; Schinke, E.; Böttcher, H. Heterocyclen aus CH-Aciden Nitrilen, VIII. 2-Amino-Thiophene aus Methylenaktiven Nitrilen, Carbonylverbindungen und Schwefel. *Chem. Ber.* 1966, 99, 94–100.

44. Puterová, Z.; Krutová, A.; Végh, D. Gewald reaction synthesis, properties and applications of substituted 2-aminothiophenes. *Arkivoc* 2010, 2010, 209–46.

45. Sedlák, M.; Pravda, M.; Staud, F.; Kubicová, L.; Týcová, K.; Ventura, K. Synthesis of pH-sensitive amphotericin B–poly(ethylene glycol) conjugates and study of their controlled release in vitro. *Bioorg. Med. Chem.* 2007, 15, 4069–76.

46. Nogueira, C.W.; Barbosa, N.V.; Rocha, J.B.T. Toxicology and pharmacology of synthetic organoselenium compounds: An update. *Arch. Toxicol.* 2021, 95, 1179–226.

47. Gallo-Rodriguez, C.; Rodriguez, J.B. Organoselenium Compounds in Medicinal Chemistry. *ChemMedChem* 2024, 19, e202400063.

48. Rubio-Hernández, M.; Alcolea, V.; Pérez-Silanes, S. Potential of sulfur-selenium isosteric replacement as a strategy for the development of new anti-chagasic drugs. *Acta Trop.* 2022, 233, 106547.

49. Pedreira, J.G.B.; Silva, R.R.; Noël, F.G.; Barreiro, E.J. Effect of S–Se Bioisosteric Exchange on Affinity and Intrinsic Efficacy of Novel N-acylhydrazone Derivatives at the Adenosine A2A Receptor. *Molecules* 2021, 26, 7364.

50. Gong, L.; Kang, J. Drug target deconvolution by chemical proteomics. *Se Pu* 2020, 38, 877–9.

51. Wilkinson, I.V.L.; Terstappen, G.C.; Russell, A.J. Combining experimental strategies for successful target deconvolution. *Drug Discov. Today.* 2020, 25, 1998–2005.

52. Chen, H.; King, F.J.; Zhou, B.; Wang, Y.; Canedy, C.J.; Hayashi, J.; et al. Pache, L.; Wong, J.L.; et al. Drug target prediction through deep learning functional representation of gene signatures. *Nat. Commun.* 2024, 15, 1853.